BioArchitecture 2:6, 220–227; November/December 2012; © 2012 Landes Bioscience

Microtubule dynamics regulation contributes to endothelial morphogenesis

Karen S. Lyle,[†] Jose A. Corleto[‡] and Torsten Wittmann*

Department of Cell and Tissue Biology; University of California at San Francisco; San Francisco, CA USA

Current Affiliations: [†]Genentech; South San Francisco, CA USA; [‡]Department of Anesthesiology; University of California at San Diego; San Diego, CA USA

Keywords: microtubule dynamics, endothelial cells, in vitro angiogenesis, cell migration, CLASP2, nocodazole, blebbistatin, cytoskeleton

Because little is known how microtubules contribute to cell migration in a physiological three-dimensional environment, we analyzed microtubule function and dynamics during in vitro angiogenesis in which endothelial cells form networks on a reconstituted basement membrane. Endothelial network formation resulted from distinct cell behaviors: matrix reorganization by myosin-mediated contractile forces, and active cell migration along reorganized, bundled matrix fibers. Inhibition of microtubule dynamics inhibited persistent cell migration, but not matrix reorganization. In addition, microtubule polymerization dynamics and CLASP2-binding to microtubules were spatially regulated to promote microtubule growth into endothelial cell protrusions along matrix tension tracks. We propose that microtubules counteract contractile forces of the cortical actin cytoskeleton and are required to stabilize endothelial cell protrusions in a soft three-dimensional environment.

Introduction

The basic mechanism of adherent cell migration in a two-dimensional (2D) environment has been studied extensively, and is thought to predominantly rely on a coordinated cycle of actin polymerization-mediated protrusion, integrin-mediated adhesion and cell body translocation resulting from actomyosin contractility.[1] However, in most cells directional migration also requires an intact microtubule cytoskeleton.[2] Microtubules are rigid cytoskeletal polymers of α/β-tubulin dimers that stochastically switch between phases of growth and shortening, a non-equilibrium polymerization behavior referred to as dynamic instability. In many cell types such as fibroblasts and epithelial cells migrating on a 2D surface, microtubules are preferentially oriented toward the front of the cell through regulated interactions with the cortical cytoskeleton. Such microtubule interactions with the cell cortex are likely mediated by a class of proteins that specifically associate with growing microtubule ends, and may stabilize microtubules by forming dynamic connections with the actin cytoskeleton or near adhesion sites.[3-7] Cells migrating in 2D lose directional polarity and cease migration when microtubule dynamics are inhibited, possibly due to disrupted Rho GTPase signaling networks required for establishment or maintenance of directional polarity.[2,8-10]

In a physiological three-dimensional (3D) environment, however, cell shape changes and interactions with the extracellular matrix are considerably more complex. Migrating cells may employ additional alternative modes of translocation,[11] and the function and regulation of the microtubule cytoskeleton during cell migration in a 3D extracellular matrix is incompletely understood. Cells squeezing through a meshwork of extracellular matrix may utilize a more amoeboid form of migration during which microtubule organization is entirely different,[12] and frequently adapt collective modes of migration, for example during the sprouting of new blood vessels during angiogenesis.[11] To analyze the role of dynamic microtubules in a more physiological cell migration model, we employed a widely used in vitro angiogenesis assay. Primary endothelial cells grown on top of a compliant reconstituted basement membrane matrix reorganize into a capillary-like network within hours. Because cells are not suspended within the Matrigel matrix, this system is a hybrid between 2D and 3D. Nevertheless, endothelial cells experience a pliable, physiological environment, which recapitulates many aspects of angiogenesis in vivo.[13,14] Here, we propose that spatial regulation of microtubule dynamics promotes the formation of microtubule bundles in endothelial cell protrusions along tension-induced aligned matrix fibers, and that these microtubule bundles are important for persistent migration by counter-acting myosin-mediated contractile forces.

Results and Discussion

Endothelial cell migration along matrix tension tracks requires dynamic microtubules. To analyze endothelial network formation dynamics, we observed HUVEC primary endothelial cells cultured on a reconstituted Matrigel basement membrane by

*Correspondence to: Torsten Wittmann; Email: torsten.wittmann@ucsf.edu
Submitted: 09/04/12; Revised: 09/21/12; Accepted: 09/21/12
http://dx.doi.org/10.4161/bioa.22190

phase contrast time-lapse microscopy for up to 12 h. In control HUVECs, different cell behaviors contributed to endothelial network formation (**Fig. 1A**; **Vid. S1**). Cells adhered and spread on the Matrigel substrate within ~30 min after plating. After 2–3 h, most cells had formed small clusters, and contractile forces between cell clusters resulted in reorganization of the extracellular matrix and in the alignment of matrix fibers.[15] These tension tracks were clearly visible by phase contrast microscopy, and typically formed between two opposing cells (**Fig. 1A and D**; **Vid. S1**). Individual cells responded to this mechanical stimulus by forming long thin protrusions along such bundles of aligned matrix fibers (**Fig. 1D**).

DIC microscopy at higher spatial and temporal resolution around 4–6 h after plating when cells were most migratory confirmed that protrusions resulted from active cell migration along matrix fiber bundles, and were not simply the result of cell stretching by opposing pulling forces on the matrix (**Fig. 2A**). Cells repeatedly elongated and retracted along these aligned matrix fibers indicating that the generation of matrix tension tracks and subsequent migration along these tracks represent distinct cell behaviors contributing to endothelial network formation. Eventually, cell migration along matrix tracks resulted in cell-cell contact formation of opposing cells to form a thin endothelial cord. Depending on cell density and network topology, these initial cords were either enforced by the migration of additional cells along the cord or disintegrated as a result of collective pulling forces on the matrix. This network consolidation coincided with a gradual disappearance of matrix tension tracks at later time points (**Fig. 1F**).

As expected, matrix remodeling depended on actomyosin contractility. Myosin II family motors localize to the endothelial cortical cytoskeleton and blebbistatin, a myosin II inhibitor, largely abolished tension track formation (**Fig. 1E**).[16,17] As a result blebbistatin-treated cells remained dispersed and failed to organize into a cell network (**Fig. 1C; Vid. S3**). However, blebbistatin-treated cells remained motile and formed many, highly branched, randomly oriented protrusions. Although these cells produced abundant lamellipodia, cell protrusions did not continue to extend in the absence of tension tracks (**Fig. 2C**).

To investigate the role of dynamic microtubules during endothelial network formation, we treated HUVEC cells with a range of low nocodazole concentrations. 100 nM nocodazole did not depolymerize microtubules, but effectively stopped intracellular microtubule polymerization as judged by the disappearance of EB1-EGFP comets, a marker of growing microtubule ends (**Fig. 3A**).[18,19] Yet, 100 nM nocodazole severely disrupted endothelial network formation (**Fig. 1B; Vid. S2**). As expected, cells became more contractile and the number of matrix tension tracks increased significantly in 100 nM nocodazole-treated cells (**Fig. 1E**).[20] However, cells failed to productively migrate along these tracks, which resulted in more tension tracks remaining in nocodazole-treated cultures at later time points (**Fig. 1B and F**).

Analysis of DIC microscopy time-lapse sequences further demonstrated that although nocodazole-treated cells were still protrusive, the persistency of protrusions along tension tracks was substantially decreased (**Fig. 2D and E**). The average life time of a protrusion phase in 100 nM nocodazole was decreased about three-fold as compared with control cells. Although it has been shown previously that microtubule depolymerization or inhibition of microtubule dynamics disrupts endothelial network formation,[15,21,22] our results demonstrate that dynamic remodeling of the microtubule network is specifically required for persistent cell migration along aligned matrix fibers, but not for the generation of endothelial cell pulling forces on the matrix.

Microtubule dynamics are spatially regulated in endothelial cells migrating along matrix tension tracks. To analyze how microtubules contributed to protrusion persistency, we first fixed and stained F-actin and microtubules in control and nocodazole-treated cells 4–6 h after plating on Matrigel (**Fig. 3B**). Control cells stretched along matrix tension tracks and always contained abundant parallel microtubule arrays that typically extended into the very tip of the protrusion. Cells treated with 100 nM nocodazole still contained numerous microtubules in the cell body confirming that this low nocodazole concentration was not sufficient to completely depolymerize microtubules even after prolonged incubation. However, microtubules in nocodazole-treated cells appeared disorganized and did not extend into cell protrusions (**Fig. 3B**). This indicated that microtubule polymerization is regulated differently in the cell body compared with protrusions along tension tracks.

To test this directly, we analyzed microtubule dynamics by spinning disk confocal live cell microscopy. We used EB1-EGFP as a marker of growing microtubule plus ends because microtubules were too dense in these protrusions to directly observe dynamic microtubules. Dual-wavelength imaging in combination with mCherry-actin revealed that microtubules actively grew into HUVEC cell protrusions (**Fig. 3C**). Although EB1-EGFP-labeled growing microtubule ends were distributed throughout the cell, the direction of microtubule growth in protrusions along tension tracks was almost exclusively toward the distal end of the protrusion (**Figs. 3D and 4A**; **Vid. S4**). Occasionally, we observed growing microtubule ends that bumped into and deformed the membrane at the distal tip of the protrusion (**Fig. 3D**). Because microtubules have a high bending rigidity,[23] this suggests that microtubules may mechanically contribute to protrusion stability in endothelial cells migrating along matrix fiber tracks in a soft 3D environment.

To determine whether microtubule dynamics were spatially regulated in endothelial cells migrating along tension tracks we employed automated tracking of EB1-EGFP comets in time-lapse sequences acquired at high temporal resolution (**Fig. 4A**; **Vid. S4**).[4,24] This analysis was technically challenging due to optical aberrations resulting from the thick Matrigel layer, and the majority of cells not being parallel to the focal plane. Nevertheless, we consistently observed that the microtubule growth rate was significantly higher in endothelial cell protrusions along tension tracks compared with the cell body (**Fig. 4B**). Although such differences could in principle result from different microtubule network geometries in cell body and protrusion, our recent, detailed analysis of microtubule dynamics in epithelial cells in 3D tissue culture indicated that this is not the case.[25] Analysis of the correlation between EB1-EGFP track length and

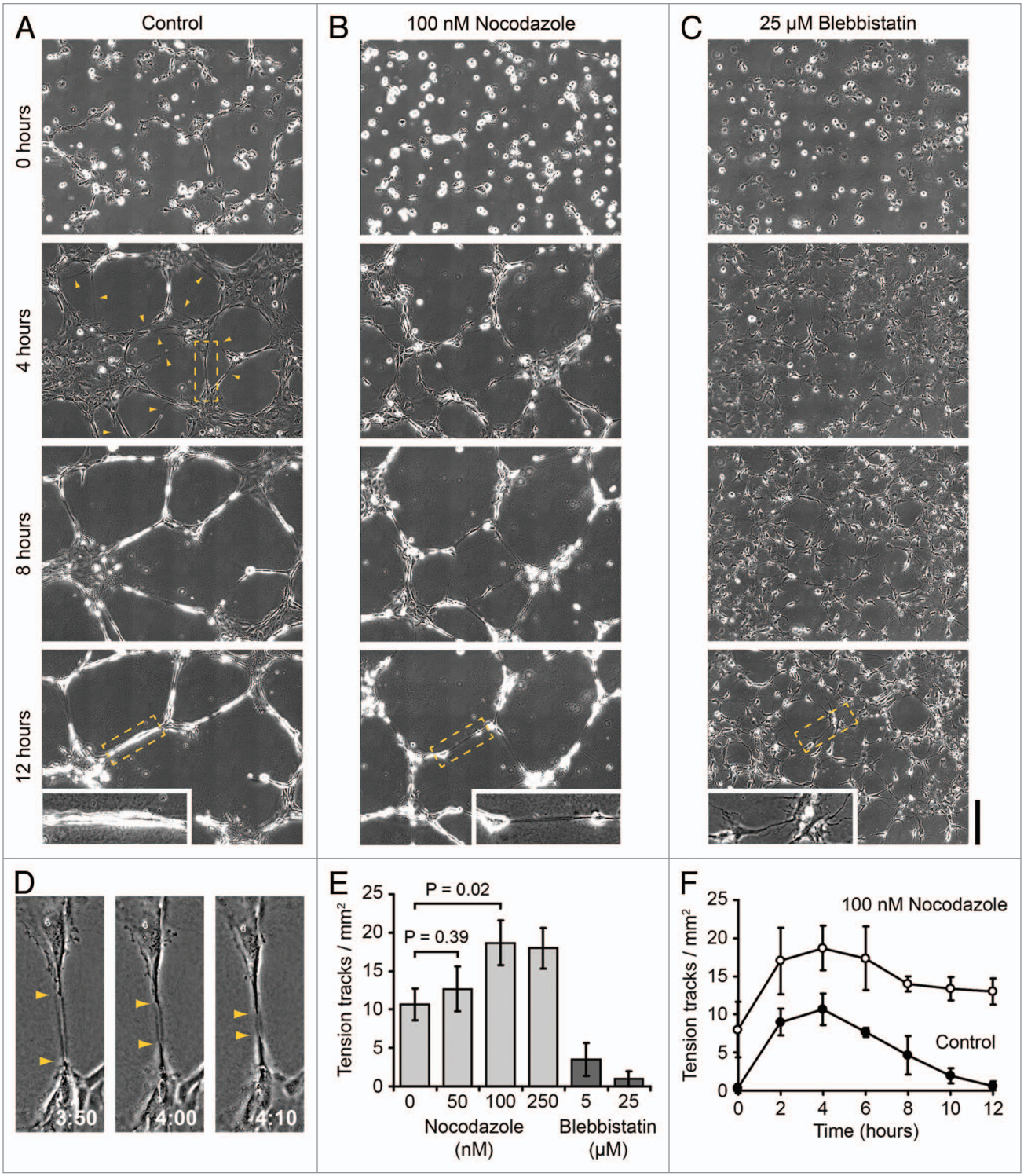

Figure 1. Endothelial network formation requires dynamic microtubules and myosin-mediated contractility. Individual images from time-lapse sequences of network formation of control HUVEC primary endothelial cells (**A**), and cells in the presence of 100 nM nocodazole (**B**) or 25 μM blebbistatin (**C**). Scale bar, 200 μm. Arrowheads in (**A**), 4 h, indicate tension tracks in the control. Insets in the 12 h time-point are higher magnification. The control inset shows a cord of endothelial cells, the nocodazole inset shows a remaining tension track. Each image is stitched from 36 individual images. (**D**) Magnification of the image region outlined by the dashed box in (**A**), 4 h, illustrating extension formation of the two opposing cells along a tension track in the matrix. Arrowheads indicate the tips of the cell protrusions. Time stamp is hours and minutes. (**E**) Quantification of the density of tension tracks 4 h after cell plating on Matrigel in the presence of increasing concentrations of nocodazole or blebbistatin. P values of relevant comparisons are indicated on the graph. (**F**) Tension track density as a function of time during endothelial network formation in control and 100 nM nocodazole-treated cells. Error bars in (**E and F**) indicate standard deviation from three independent experiments.

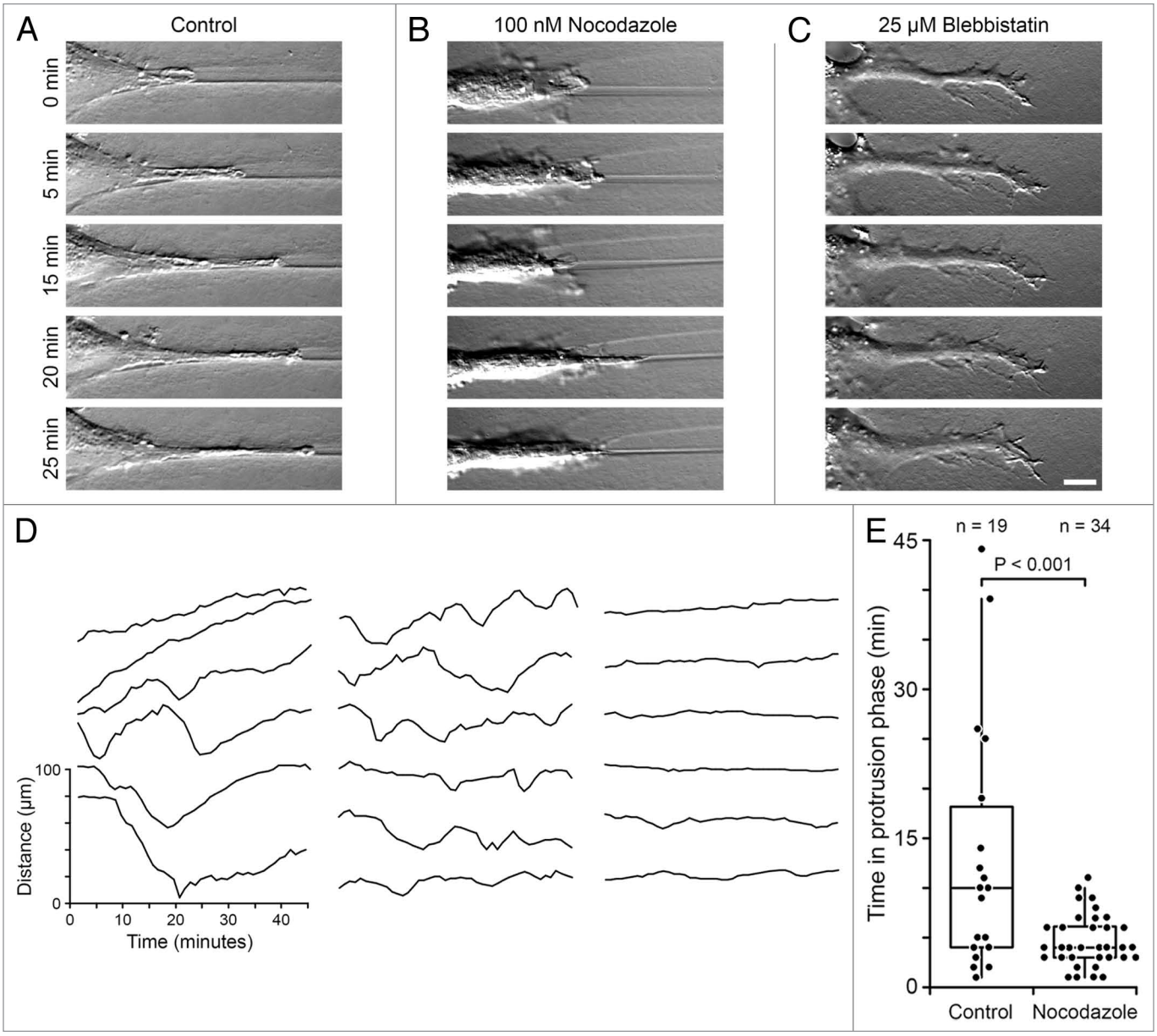

Figure 2. Endothelial cell migration along matrix tension tracks. Images from DIC time-lapse sequences of protrusion dynamics in control HUVECs (**A**), and cells in the presence of 100 nM nocodazole (**B**) or 25 μM blebbistatin (**C**). Scale bar, 10 μm. Note the absence of aligned matrix fibers in blebbistatin-treated cells. (**D**) Representative displacement traces of the protrusion tip as a function of time of six different control, nocodazole-, and blebbistatin-treated cells each, indicating that protrusions collapse more frequently in nocodazole-treated cells. (**E**) Quantification of the length of protrusion phases along matrix tension tracks in control and 100 nM nocodazole-treated cells from eight 45 min time-lapse sequences per condition. Each circle represents a protrusion phase. Note that because protrusion phases are shorter in nocodazole-treated cells, a larger number of events is measured in the same time period.

measured growth rate demonstrated that although microtubule network geometry contributes to the spread of measured growth rates, it does not account for systematic differences in different intracellular domains.[25] In addition, we did not observe a measurable growth rate increase in growth factor-induced protrusions in epithelial cells that appear morphologically quite similar to endothelial cells migrating along tension tracks.[25] In this regard it is interesting to note that low doses of microtubule perturbing drugs increase microtubule dynamics in endothelial cells,[21,22,26] an effect that also is unique to endothelial cells. Together, these observations suggest endothelial cell-specific mechanisms of microtubule regulation, and it will be interesting to see whether this can be therapeutically exploited.

We and others have shown that CLASPs are microtubule plus-end-tracking proteins that are partially responsible for microtubule interactions with the cortical cytoskeleton in migrating cells.[7,27-29] In addition, microtubule association of CLASP proteins is spatiotemporally controlled in migrating cells, and dephosphorylation of CLASPs near the leading edge locally increases CLASP-microtubule binding likely as a result

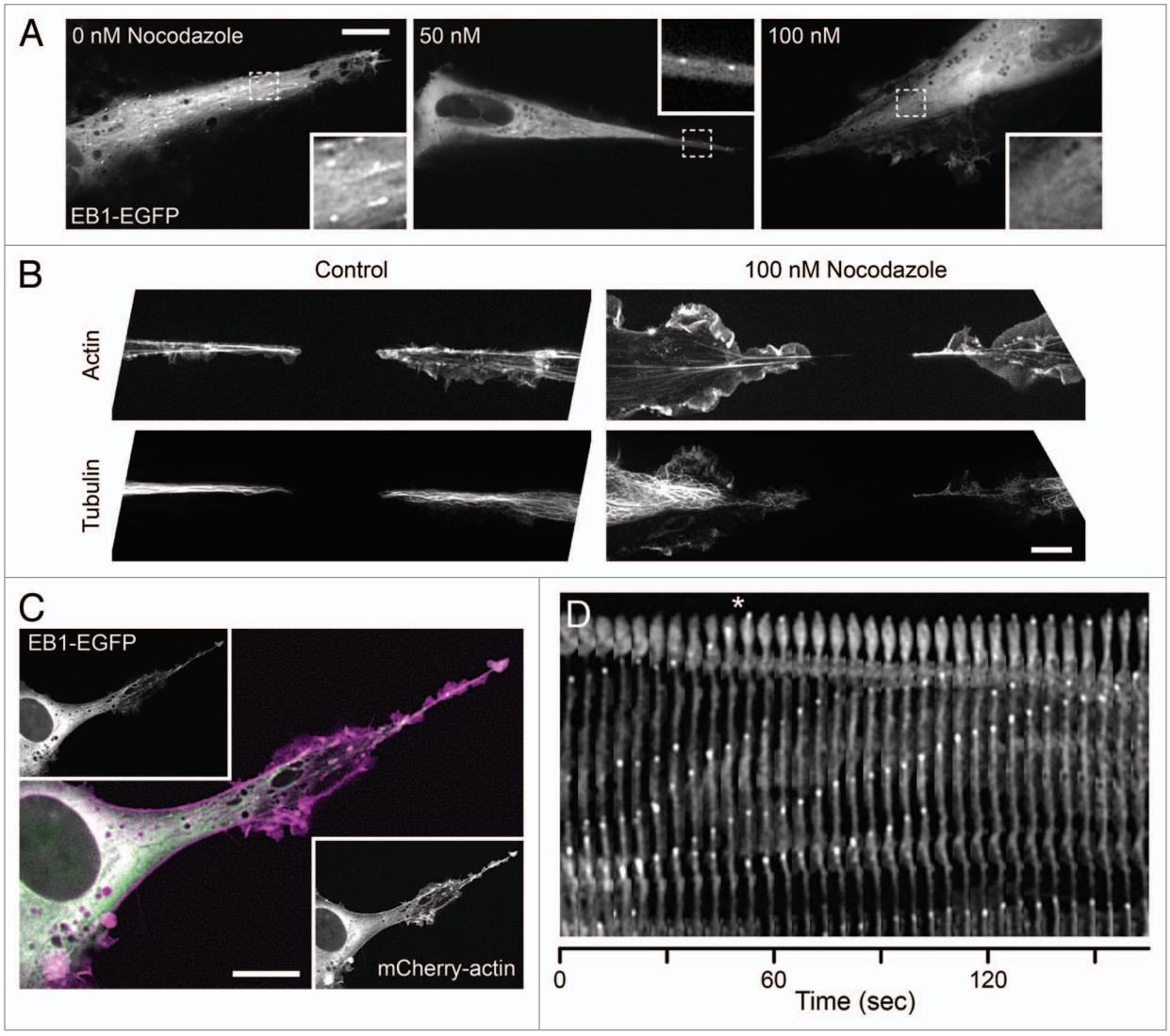

Figure 3. Microtubule organization and dynamics in endothelial cells migrating along tension tracks. (**A**) EB1-EGFP localization in the presence of low concentrations of nocodazole in endothelial cells during network formation. Growing microtubule ends are still visible at 50 nM nocodazole, but are completely absent at 100 nM. (**B**) F-actin and microtubule immunofluorescence of opposing endothelial cell protrusions along tension tracks in control and nocodazole-treated cells. (**C**) Image from a time-lapse sequence of a cell expressing EB1-EGFP and mCherry-actin. Insets show individual channels. (**D**) Kymograph of EB1-EGFP in the thin distal part of the protrusion of the cell shown in (**C**) demonstrating persistent microtubule growth toward the distal tip of the protrusion. The asterisk indicates deformation of the distal protrusion tip by a growing microtubule.

of local GSK3β inactivation.[4] To test whether such a gradient of CLASP-microtubule binding also existed in endothelial cells migrating along tension tracks, we analyzed the localization of EGFP-CLASP2. Indeed, although EGFP-CLASP2 evidently bound along microtubule ends in the protrusion, in contrast to EB1-EGFP, EGFP-CLASP2 was completely absent from microtubules in the cell body (**Fig. 4C**). The bright perinuclear signal is Golgi-associated EGFP-CLASP2 that occurs independent of microtubules.[30] EGFP-CLASP2(9 × S/A) in which all GSK3β phosphorylation sites were replaced with non-phosphorylatable alanine residues associated with microtubule ends equally well in the cell body and the protrusion,[4] confirming that the spatial gradient of CLASP2 microtubule-binding resulted from differences in the GSK3β-mediated CLASP2 phosphorylation state.

In conclusion, our data support a mechanism in which the different dynamic and mechanical properties of the microtubule and actin cytoskeletons cooperate during persistent endothelial cell migration along matrix tracks in a physiological environment. We propose that spatiotemporal regulation of microtubule dynamics results in active microtubule growth into elongating protrusions, and stabilization of these microtubules through interactions of distal microtubule parts with the cortical cytoskeleton near the protrusion tip. This is likely mediated by microtubule plus end-tracking proteins that bind to growing microtubule ends through interactions with EB1.[18,25] Because adhesion as well as the resistance to contractile forces of a soft 3D extracellular matrix is probably small compared with adhesion on a 2D rigid coverslip, microtubules may play a more important role in 3D.

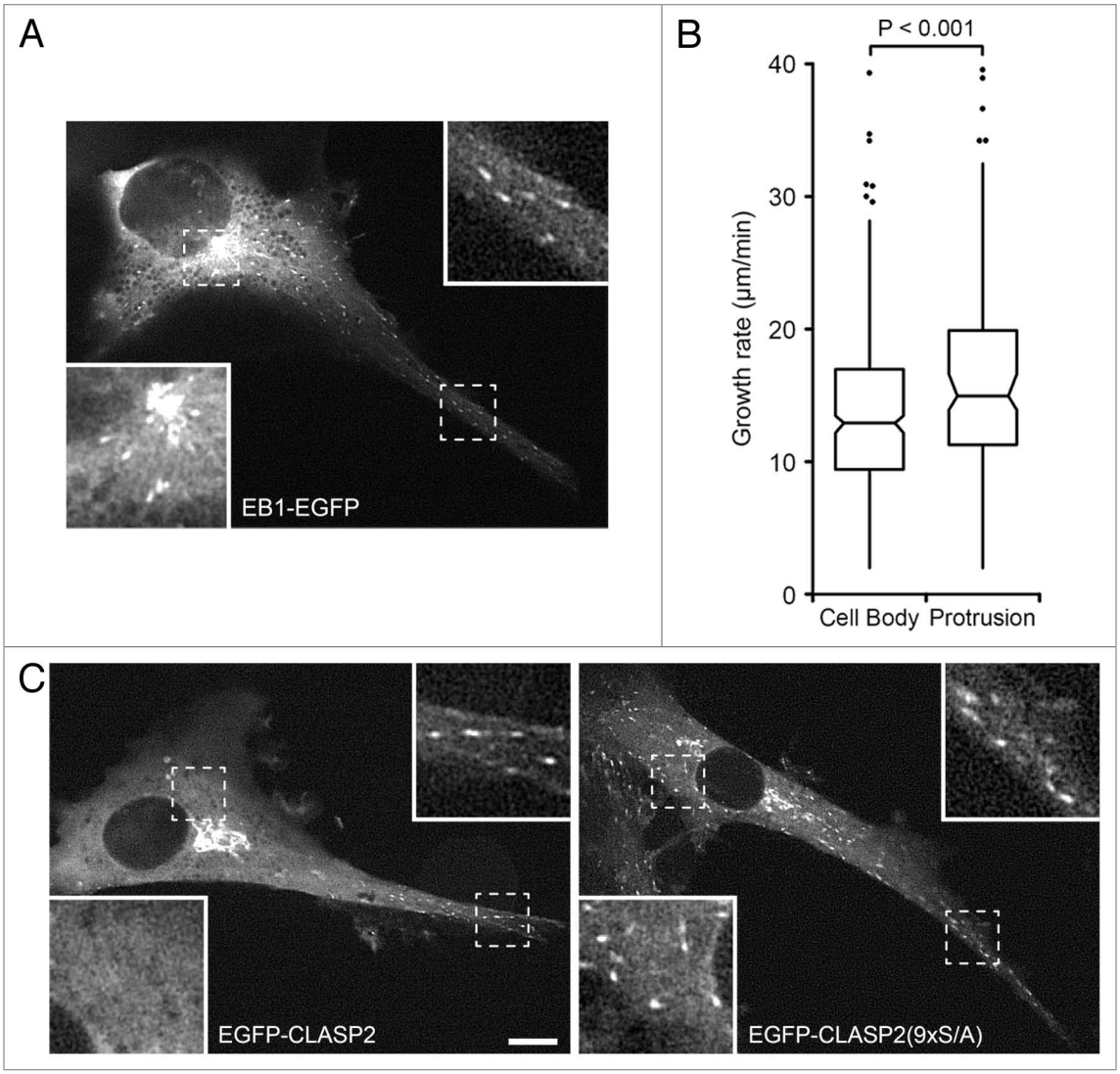

Figure 4. Spatiotemporal microtubule regulation during endothelial cell network formation. (**A**) Image of a time-lapse sequence of an EB1-EGFP expressing cell acquired at 2 frames per second. EB1-EGFP positive, growing microtubule ends are distributed throughout the cell. Insets show the regions in the cell body and the protrusion indicated by dashed boxes at higher magnification. (**B**) Box-and-whisker plot of microtubule growth rates analyzed by EB1-EGFP comet tracking in the cell body compared with the cell protrusion. Outliers are indicated by circles. Notches indicate 95% confidence intervals. n = 300 microtubules. (**C**) Distribution of wild-type EGFP-CLASP2 or non-phosphorylatable EGFP-CLASP2(9 × S/A) in which GSK3β phosphorylation sites are replaced with alanines. This indicates spatial regulation of wild-type EGFP-CLASP2 in endothelial cells in a 3D matrix. Insets show the regions in the cell body and the protrusion indicated by dashed boxes at higher magnification. Scale bars, 10 μm.

Microtubules crosslinked to the cell cortex may be required to counteract actomyosin contractility and prevent protrusion collapse. This is supported by the observation that remaining microtubules in protrusions of nocodazole-treated cells often appeared buckled (**Fig. 3B**), which indicates the presence of compressive forces on microtubules as a result of protrusion retraction. This is consistent with a tensegrity model for endothelial cell migration along matrix fiber tracks in 3D in which rigid microtubule bundles act as compression elements that counteract actomyosin-mediated contractile forces.[31,32] In addition, microtubule growth into long endothelial cell protrusions along matrix tension tracks is likely essential for organelle redistribution and forward transport,[25] and may be required for contact formation during endothelial cord formation.[33]

Materials and Methods

Cell culture. Pooled HUVECs (Invitrogen, Cascade Biologics) were cultured in Medium 200 and Low Serum Growth Supplement (Invitrogen, Cascade Biologics) at 37°C and 5% CO_2. For 3D angiogenesis assays, a thin layer of BD Matrix Growth Factor Reduced Matrigel (BD Biosciences) was spread onto the bottom surface of either a 2-well #1 Lab-Tek chambered coverglass (Nalgene Nunc International) or a 35 mm #1 glass bottom dish (MaTek Corporation). The Matrigel was allowed to solidify for ~15 min at 37°C, 5% CO_2 before plating ~20,000 cells/cm^2. After the cells adhered (~30 min after plating), medium and unattached cells were aspirated and replaced with

fresh medium, containing 25 mM HEPES (Gibco) and indicated concentrations of nocodazole (Sigma-Aldrich), (-)-blebbistatin (Sigma-Aldrich) or DMSO as a vehicle control. For live cell imaging, chambers were sealed with silicone vacuum grease (Dow Corning) to prevent media evaporation.

Adenoviral vectors and transduction. mCherry-actin, EB1-EGFP and EGFP-CLASP2 expressing adenovirus particles were produced using the AdEasy system (Agilent Technologies) as described.[34] HUVECs were infected with recombinant adenoviruses for 1 h and allowed to express proteins for 18 h before plating on Matrigel. For double infections, both viruses were added simultaneously.

Immunofluorescence. HUVECs in 3D cultures were washed in warm PBS, briefly fixed in 0.25% glutaraldehyde in BRB80 (80 mM K-PIPES, 1 mM EGTA, 1 mM $MgCl_2$) and then fixed for 5 min in the same fixative also containing 0.1% Triton X-100. Glutaraldehyde autofluorescence was quenched in 0.2% sodium borohydride in PBS. Cells were stained using standard protocols with a rat anti-tubulin antibody (MCA77G, Serotec) and fluorescently labeled phalloidin (Invitrogen) and stored in PBS containing 0.1% sodium azide.

Image acquisition and analysis. EB1-EGFP, EGFP-CLASP2 and mCherry-actin dynamics were imaged at 37°C with a 60× NA 1.20 (Plan Apo VC; Nikon) water immersion objective lens on an inverted microscope system (TE-2000 PFS; Nikon) equipped with a spinning-disk confocal unit (CSU10; Yokogawa) with 200 mW, 488 nm and 561 nm solid-state lasers (LMM5; Spectral Applied Research), electronic shutters, a cooled charge-coupled device camera (Cool-SNAP HQ2; Photometrics), and controlled by NIS Elements software (Nikon). Microtubule growth rates were determined by computational tracking of EB1-EGFP comets in time-lapse sequences.[24] Comet detection was improved by reducing low frequency background variation with a homomorphic filter in the frequency domain (MetaMorph; Molecular Devices). Only tracks existing for at least 5 frames (2.5 sec) were used for analysis to bias against microtubules that did grow at an angle relative to the plane of focus. A 60× NA 1.45 oil immersion lens (Plan Apo TIRF; Nikon) was used to image cell extensions by DIC microscopy and for immunofluorescence. To measure protrusion dynamics in DIC images, we used the manual tracking function in NIS Elements (Nikon). A 40× objective lens (Plan Fluor ADM/ELWD; Nikon), and the large image function in NIS Elements were used to collect 6 × 6 stitched phase contrast time-lapse sequences. In these high-resolution phase contrast images, matrix tension tracks were readily visible as dark striations and were counted at indicated time points. Statistical analysis was performed in Excel (Microsoft) using the Analyze-it plug-in for Excel (Analyze-it Software, Ltd). Box-and-whisker plots show the median, the 1st and 3rd quartile (box), with whiskers extending to the furthest observations within ± 1.5 times the interquartile ranges of the 1st or 3rd quartile. P values were calculated from two-sample equal variance, 2-tailed t-tests. Images for presentation in figures and movies were contrast-enhanced as described.[29]

Acknowledgments

This work was supported by American Heart Association Scientist Development Grant 0730032N to T.W. and NIH/NIDCR training grant 5T32DE007306 to K.L. Research was conducted in a facility constructed with support from the NIH/NCRR Research Facilities Improvement Program grant C06 RR16490.

Supplemental Materials

Supplemental materials may be found here:
www.landesbioscience.com/journals/BioArchitecture/article/22335

References

1. Vicente-Manzanares M, Choi CK, Horwitz AR. Integrins in cell migration--the actin connection. J Cell Sci 2009; 122:199-206; PMID:19118212; http://dx.doi.org/10.1242/jcs.018564
2. Wittmann T, Waterman-Storer CM. Cell motility: can Rho GTPases and microtubules point the way? J Cell Sci 2001; 114:3795-803; PMID:11719546
3. Akhmanova A, Steinmetz MO. Tracking the ends: a dynamic protein network controls the fate of microtubule tips. Nat Rev Mol Cell Biol 2008; 9:309-22; PMID:18322465; http://dx.doi.org/10.1038/nrm2369
4. Kumar P, Lyle KS, Gierke S, Matov A, Danuser G, Wittmann T. GSK3beta phosphorylation modulates CLASP-microtubule association and lamella microtubule attachment. J Cell Biol 2009; 184:895-908; PMID:19289791; http://dx.doi.org/10.1083/jcb.200901042
5. Wu X, Kodama A, Fuchs E. ACF7 regulates cytoskeletal-focal adhesion dynamics and migration and has ATPase activity. Cell 2008; 135:137-48; PMID:18854161; http://dx.doi.org/10.1016/j.cell.2008.07.045
6. Rodriguez OC, Schaefer AW, Mandato CA, Forscher P, Bement WM, Waterman-Storer CM. Conserved microtubule-actin interactions in cell movement and morphogenesis. Nat Cell Biol 2003; 5:599-609; PMID:12833063; http://dx.doi.org/10.1038/ncb0703-599
7. Stehbens S, Wittmann T. Targeting and transport: How microtubules control focal adhesion dynamics. J Cell Biol 2012; 198:481-9; PMID:22908306; http://dx.doi.org/10.1083/jcb.201206050
8. Liao G, Nagasaki T, Gundersen GG. Low concentrations of nocodazole interfere with fibroblast locomotion without significantly affecting microtubule level: implications for the role of dynamic microtubules in cell locomotion. J Cell Sci 1995; 108:3473-83; PMID:8586659
9. Waterman-Storer CM, Worthylake RA, Liu BP, Burridge K, Salmon ED. Microtubule growth activates Rac1 to promote lamellipodial protrusion in fibroblasts. Nat Cell Biol 1999; 1:45-50; PMID:10559863; http://dx.doi.org/10.1038/9018
10. Birkenfeld J, Nalbant P, Yoon SH, Bokoch GM. Cellular functions of GEF-H1, a microtubule-regulated Rho-GEF: is altered GEF-H1 activity a crucial determinant of disease pathogenesis? Trends Cell Biol 2008; 18:210-9; PMID:18394899; http://dx.doi.org/10.1016/j.tcb.2008.02.006
11. Friedl P. Prespecification and plasticity: shifting mechanisms of cell migration. Curr Opin Cell Biol 2004; 16:14-23; PMID:15037300; http://dx.doi.org/10.1016/j.ceb.2003.11.001
12. Eddy RJ, Pierini LM, Maxfield FR. Microtubule asymmetry during neutrophil polarization and migration. Mol Biol Cell 2002; 13:4470-83; PMID:12475966; http://dx.doi.org/10.1091/mbc.E02-04-0241
13. Vernon RB, Sage EH. Between molecules and morphology. Extracellular matrix and creation of vascular form. Am J Pathol 1995; 147:873-83; PMID:7573362
14. Kleinman HK, Martin GR. Matrigel: basement membrane matrix with biological activity. Semin Cancer Biol 2005; 15:378-86; PMID:15975825; http://dx.doi.org/10.1016/j.semcancer.2005.05.004
15. Vernon RB, Angello JC, Iruela-Arispe ML, Lane TF, Sage EH. Reorganization of basement membrane matrices by cellular traction promotes the formation of cellular networks in vitro. Lab Invest 1992; 66:536-47; PMID:1374138
16. Limouze J, Straight AF, Mitchison T, Sellers JR. Specificity of blebbistatin, an inhibitor of myosin II. J Muscle Res Cell Motil 2004; 25:337-41; PMID:15548862; http://dx.doi.org/10.1007/s10974-004-6060-7
17. Fischer RS, Gardel M, Ma X, Adelstein RS, Waterman CM. Local cortical tension by myosin II guides 3D endothelial cell branching. Curr Biol 2009; 19:260-5; PMID:19185493; http://dx.doi.org/10.1016/j.cub.2008.12.045
18. Kumar P, Wittmann T. +TIPs: SxIPping along microtubule ends. Trends Cell Biol 2012; 22:418-28; PMID:22748381; http://dx.doi.org/10.1016/j.tcb.2012.05.005
19. Honoré S, Pagano A, Gauthier G, Bourgarel-Rey V, Verdier-Pinard P, Civiletti K, et al. Antiangiogenic vinflunine affects EB1 localization and microtubule targeting to adhesion sites. Mol Cancer Ther 2008; 7:2080-9; PMID:18645018; http://dx.doi.org/10.1158/1535-7163.MCT-08-0156

20. Bershadsky A, Chausovsky A, Becker E, Lyubimova A, Geiger B. Involvement of microtubules in the control of adhesion-dependent signal transduction. Curr Biol 1996; 6:1279-89; PMID:8939572; http://dx.doi.org/10.1016/S0960-9822(02)70714-8
21. Pasquier E, Honore S, Pourroy B, Jordan MA, Lehmann M, Briand C, et al. Antiangiogenic concentrations of paclitaxel induce an increase in microtubule dynamics in endothelial cells but not in cancer cells. Cancer Res 2005; 65:2433-40; PMID:15781659; http://dx.doi.org/10.1158/0008-5472.CAN-04-2624
22. Pourroy B, Honoré S, Pasquier E, Bourgarel-Rey V, Kruczynski A, Briand C, et al. Antiangiogenic concentrations of vinflunine increase the interphase microtubule dynamics and decrease the motility of endothelial cells. Cancer Res 2006; 66:3256-63; PMID:16540678; http://dx.doi.org/10.1158/0008-5472.CAN-05-3885
23. Hawkins T, Mirigian M, Selcuk Yasar M, Ross JL. Mechanics of microtubules. J Biomech 2010; 43:23-30; PMID:19815217; http://dx.doi.org/10.1016/j.jbiomech.2009.09.005
24. Matov A, Applegate K, Kumar P, Thoma C, Krek W, Danuser G, et al. Analysis of microtubule dynamic instability using a plus-end growth marker. Nat Methods 2010; 7:761-8; PMID:20729842; http://dx.doi.org/10.1038/nmeth.1493
25. Gierke S, Wittmann T. EB1-recruited microtubule +TIP complexes coordinate protrusion dynamics during 3D epithelial remodeling. Curr Biol 2012; 22:753-62; PMID:22483942; http://dx.doi.org/10.1016/j.cub.2012.02.069
26. Bazaa A, Pasquier E, Defilles C, Limam I, Kessentini-Zouari R, Kallech-Ziri O, et al. MVL-PLA2, a snake venom phospholipase A2, inhibits angiogenesis through an increase in microtubule dynamics and disorganization of focal adhesions. PLoS ONE 2010; 5:e10124; PMID:20405031; http://dx.doi.org/10.1371/journal.pone.0010124
27. Akhmanova A, Hoogenraad CC, Drabek K, Stepanova T, Dortland B, Verkerk T, et al. Clasps are CLIP-115 and -170 associating proteins involved in the regional regulation of microtubule dynamics in motile fibroblasts. Cell 2001; 104:923-35; PMID:11290329; http://dx.doi.org/10.1016/S0092-8674(01)00288-4
28. Mimori-Kiyosue Y, Grigoriev I, Lansbergen G, Sasaki H, Matsui C, Severin F, et al. CLASP1 and CLASP2 bind to EB1 and regulate microtubule plus-end dynamics at the cell cortex. J Cell Biol 2005; 168:141-53; PMID:15631994; http://dx.doi.org/10.1083/jcb.200405094
29. Wittmann T, Waterman-Storer CM. Spatial regulation of CLASP affinity for microtubules by Rac1 and GSK3beta in migrating epithelial cells. J Cell Biol 2005; 169:929-39; PMID:15955847; http://dx.doi.org/10.1083/jcb.200412114
30. Efimov A, Kharitonov A, Efimova N, Loncarek J, Miller PM, Andreyeva N, et al. Asymmetric CLASP-dependent nucleation of noncentrosomal microtubules at the trans-Golgi network. Dev Cell 2007; 12:917-30; PMID:17543864; http://dx.doi.org/10.1016/j.devcel.2007.04.002
31. Brangwynne CP, MacKintosh FC, Kumar S, Geisse NA, Talbot J, Mahadevan L, et al. Microtubules can bear enhanced compressive loads in living cells because of lateral reinforcement. J Cell Biol 2006; 173:733-41; PMID:16754957; http://dx.doi.org/10.1083/jcb.200601060
32. Ingber DE, Tensegrity I. Cell structure and hierarchical systems biology. J Cell Sci 2003; 116:1157-73; PMID:12615960; http://dx.doi.org/10.1242/jcs.00359
33. Stehbens SJ, Akhmanova A, Yap AS. Microtubules and cadherins: a neglected partnership. Front Biosci 2009; 14:3159-67; PMID:19273264; http://dx.doi.org/10.2741/3442
34. Gierke S, Kumar P, Wittmann T. Analysis of microtubule polymerization dynamics in live cells. Methods Cell Biol 2010; 97:15-33; PMID:20719263; http://dx.doi.org/10.1016/S0091-679X(10)97002-7